



Research Article

Trace and Rare Earth Element Partitioning in Organic Fractions of Mudstones during the Oil Formation

Ping Gao ¹, Boyuan Li,² and Xianming Xiao ¹

¹School of Energy Resources, China University of Geosciences (Beijing), Beijing 100083, China

²Economics & Technology Research Institute, CNPC, Beijing 100724, China

Correspondence should be addressed to Xianming Xiao; xmxiao@cugb.edu.cn

Received 14 May 2022; Accepted 4 July 2022; Published 23 July 2022

Academic Editor: Yuxiang Zhang

Copyright © 2022 Ping Gao et al. This is an open access article distributed under the Creative Commons Attribution License, which permits unrestricted use, distribution, and reproduction in any medium, provided the original work is properly cited.

In order to investigate trace and rare earth element partitioning in organic fractions of mudstones, this study isolated organic fractions of mudstones, including insoluble organic fraction (kerogen), soluble organic fraction (extract), or expelled hydrocarbon (reservoir solid bitumen), and the isolated organic fractions and their corresponding whole rocks for trace and rare earth element compositions were measured. Analysis of trace and rare earth element compositions in organic fractions of lacustrine and marine mudstones revealed that mudstone kerogens were more enriched in rare earth elements (REE) and redox-sensitive trace elements (e.g., U, Mo, and Ni) relative to corresponding whole rocks. During the oil generation, middle rare earth elements (Sm-Ho), especially Eu, migrated from kerogen to extract more easily than the rest REE. The Eu was easily transferred to soluble hydrocarbon under the acidic and reducing environments formed by oil generation, resulting in the higher concentrations of Eu relative to its neighboring REE (Sm and Gd) and the pronounced positive Eu anomalies. Transition metal elements (e.g., Mo, V, Cr, Co, Ni, Cu, and Zn) also more easily released from kerogen than the rest elements, especially V and Ni. The enrichment and mobilization of trace elements in organic fractions of mudstones, such as Mo, U, V, Ni, and Ba, are closely related with their geochemical behaviors during the depositional and early diagenetic processes, providing the potential information for predicting the distribution characteristics of trace elements in the expelled hydrocarbons of mudstones (e.g., crude oil and solid bitumen) and fingerprinting of oil to source.

1. Introduction

Trace and rare earth elements are not only widely used to discriminate the paleoenvironmental reconstruction, provenance, and tectonic setting of sediments [1–17] but also employed in crude oil classifications and oil-source correlations [18–26]. In the past times, many authors had focused on the study of trace and rare earth elements in mudstone whole rocks [3–5, 12, 25]. It is well known that mudstone is mainly composed of silicate, organic, carbonate, and sulfide fractions [1]. Each fraction has its unique trace and rare earth element compositions which may represent special geological significances, for example, REE geochemical characteristics of seawater may be recorded in the carbonate fraction [1] and the core of authigenic phosphate nodules [6] in mudstones. Mudstone is the major contributor to global oil and gas [26, 27]. However, only organic fractions in mud-

stones have a direct genetic relationship with hydrocarbons, including insoluble organic fraction (kerogen) and soluble organic fraction (extract). Kerogen is the main body of sedimentary organic matter, accounting for 80–90% total organic matter. Hunt considered that 80–95% petroleum hydrocarbons were formed via the transformation of kerogens [27]. Extract is also a product of thermal degradation of kerogen, which has the most similar physical and chemical properties with the expelled hydrocarbons (e.g., crude oils and solid bitumen). A large amount of organic and inorganic compounds is included in crude oils. For a long time, biomarkers that belonged to organic compounds have played a huge role in petroleum exploration [28], whereas the use of inorganic compounds in petroleum exploration has been limited to V and Ni porphyrin complexes (e.g., DPEP and ETIO) [29, 30]. Due to the relatively high abundances of V and Ni in crude oils [19, 26], both elements

attracted more attentions in the study of trace elements in crude oils. Most recently, the role of other trace elements (e.g., REE, Pt, and Pd) in the processes of petroleum generation and migration has also received extensive attentions [24, 31–34]. However, few literatures had systematically reported trace and rare earth element partitioning in organic fractions of mudstones during the oil formation.

Through the analysis of trace and rare earth elements in organic fractions of lacustrine and marine mudstones, including kerogen, extract, or reservoir solid bitumen, this study investigated the trace and rare earth element partitioning in organic fractions of mudstones and their geological significances.

2. Sample Collection and Geological Setting

To comprehensively assess the trace and rare earth element partitioning in organic fractions of mudstones, this study collected the Lower Cretaceous lacustrine mudstones from Aer Sag, Erlian Basin, as well as the Lower Cambrian marine mudstones and the Upper Ediacaran reservoir solid bitumens from the Sichuan Basin (Figure 1). Detailed information of samples is listed in Table 1.

Aer Sag, located on the northeast margin of the Erlian Basin, covers an area of 2000 km², with 800 km² in China and the rest in Mongolia (Figure 1). Aer Sag was formed by regional rifting in the middle stage of the Yanshan movement, received the Lower Cretaceous lacustrine clastic deposits with the maximum thickness of 3800 m, and developed three major successions from top to bottom: Cenozoic, Lower Cretaceous, and Paleozoic (not drill to bottom) [35]. The Lower Cretaceous Bayanhua Group is the main body and can be divided into three formations from top to bottom: Saihantala (K_{1s}), Tengger (K_{1bt}), and Arshan (K_{1ba}). Each formation can be further subdivided into several members based on the lithology and fossil assemblages (Figure 1). During the formation and evolution of Aer Sag, four suits of dark mudstone were developed, including Saihantala Formation (K_{1s}), the 2nd member of Tengger Formation (K_{1bt}²), the 1st member of Tengger Formation (K_{1bt}¹), and Arshan Formation (K_{1ba}). Among them, K_{1s} and K_{1bt}² source rocks were still immature and could not be served as the effective source rocks, but K_{1bt}¹ and K_{1ba} source rocks were mature capable of hydrocarbon generation [36]. Previous oil-source correlation results showed that the source of major reservoirs mainly originated from K_{1bt}¹ source rocks, followed by K_{1ba} source rocks in order [36].

Sichuan Basin, located in the southwest of China, covers an area of 19 × 10⁴ km². Sichuan Basin was mainly filled with marine sediments. A complete succession of Ediacaran-Cambrian was developed in the Central Sichuan Basin [37–39]. Ediacaran was divided into two series: Lower Ediacaran Doushantuo Formation (Z_{1ds}) and Upper Ediacaran Dengying Formation (Z_{2dn}; Figure 1). Doushantuo Formation received a succession of clastic sediments. Dengying Formation developed a large suit of dolomite sediments, which can be subdivided into four members from bottom to top based on the enrichment degree of algae and structural characteristics: Z_{2dn}¹, Z_{2dn}², Z_{2dn}³, and Z_{2dn}⁴. Reservoir solid bitumens are widely developed in the Dengying

dolomite in Sichuan Basin and its peripheral areas [39–41]. Reservoir solid bitumens in this study were collected from Z_{2dn}⁴ dolomites. The black mudstones and shales of the Lower Cambrian Qiongzhusi formation (E_{1q}) were widely developed in Sichuan Basin and its peripheral areas. It had large thickness (100–400 m) [42] and was enriched in organic matter, which was considered major source rocks in Sichuan Basin [38, 39, 42–44]. Previous studies indicated that the Upper Ediacaran natural gas and reservoir solid bitumens chiefly originated from the Lower Cambrian mudstones and shales [31, 37, 40, 44].

3. Sample Pretreatment and Analytical Methods

3.1. Sample Pretreatment. For mudstones, all samples were washed by distilled water and then dried at room temperature. For reservoir solid bitumens, firstly, all bitumen-bearing dolomite samples were grounded to 3~5 mm without direct mental contact, and then solid bitumen particles were picked out by wood tool. Secondly, pure bitumen particles without dolomite veins were picked out under a microscope of magnifications of 10. Thirdly, they were washed by anhydrous ethanol under an ultrasonic bath and then dried at room temperature. Finally, mudstone and bitumen samples were grounded to 200 meshes in an agate mortar. About 40 g of the Lower Cretaceous mudstone samples, about 10 g of the Lower Cambrian mudstone samples, and about 0.2 g of pure solid bitumen samples were prepared.

All powdered lacustrine mudstone samples were extracted for 72 h using a Soxhlet apparatus and about 400 mL of dichloromethane and methanol (93 : 7 v : v). The extracted mixture and residue were then separated by a membrane filter of 0.45 μm. The extracted mixture was dried in the fume hood for three days at room temperature and pressure to obtain the extract without organic solvents. The mudstone residues were collected for kerogen isolation. Firstly, the mudstone residue was added with 6 mol/L HCl. The mixture was stirred for 90 min at 60–70°C, and then the acid solution was removed. This procedure was repeated three times to remove carbonates completely. Secondly, the carbonate-free residue was treated with 6 mol/L HCl and 40% HF. The mixture was stirred for 90 min at 60–70°C, and then the acid solution was removed. This procedure was repeated two times for fully destroying the silicates. Finally, the carbonate and silicate-free residue was leached with 3% HNO₃ to remove pyrites and other insoluble minerals. The mixture was stirred for 90 min at 60–70°C, and then the acid solution was removed. The residue was washed with distilled water several times to remove acid, froze for 10 h at -5°C and dried at <60°C in the oven. Finally, kerogen was isolated.

3.2. Analytical Methods. Total organic carbon (TOC) and rock pyrolysis analyses were conducted at state key laboratory of petroleum resources and prospecting in China University of Petroleum using the total carbon and sulfur Leco CS-230 analyzer and OGE-II oil and gas evaluation workstation, respectively. Trace and rare earth element (REE) analysis were conducted at Analytical Laboratory of

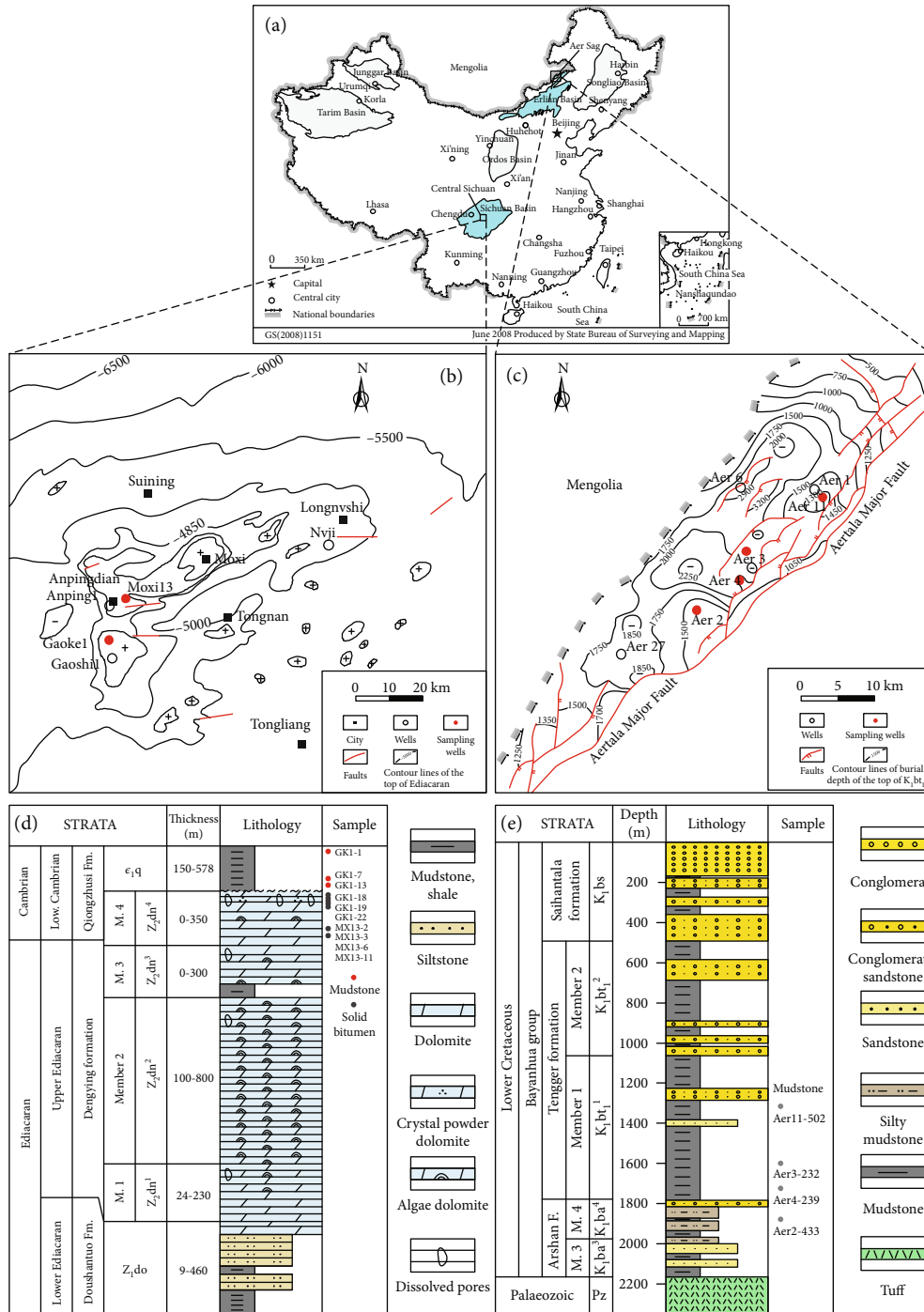


FIGURE 1: Generalized structural location map and stratigraphic column for the Central Sichuan Basin and Aer Sag in Erlian Basin. (a) The distribution of sedimentary basins in China. The structural location map of (b) the Central Sichuan Basin and (c) the Aer Sag modified after [36, 37], respectively. The stratigraphic column of (d) the Central Sichuan Basin and (e) the Aer Sag modified after [36, 42], respectively.

Beijing Research Institute of Uranium Geology using Thermo Scientific Element XR ICP-MS, respectively. The digestion procedures for trace and rare earth element detection were described by [21]. Analytical precision was better than 5% for trace elements and 10% for REE. The Ce and Eu anomalies were calculated according to [45]; i.e., $Ce/Ce^* = Ce_N / (La_N \times Pr_N)^{1/2}$, and $Eu/Eu^* = Eu_N / (Sm_N \times Gd_N)^{1/2}$, where N

refers to elemental concentrations normalized to the Post-Archean Australian Shale (PAAS; [46]).

4. Results

4.1. Bulk Geochemical Parameters. Total organic carbon (TOC), rock pyrolysis and vitrinite reflectance (R_0), or

TABLE 1: Basic information of mudstone samples in the study (sample number consisted of well name and original sampling number. See Figure 1 for the location of the wells).

Sample No.	Area	Depth/m	Formation	Rock description
Aer3-232	Aer Sag, Erlian Basin	1639.9	K ₁ bt ¹	Dark mudstone
Aer4-239		1823.5	K ₁ bt ¹	Dark mudstone
Aer2-433		1911.54	K ₁ ba ⁴	Dark mudstone
Aer11-502		1330.84	K ₁ bt ¹	Dark mudstone
GK1-1		4895.99	Є ₁ q	Black mudstone
GK1-7	Sichuan Basin	4981.37~4981.47	Є ₁ q	Black mudstone
GK1-13		4985	Є ₁ q	Black mudstone
GK1-18		4989.28~4989.57	Z ₂ dn ⁴	Bitumen-bearing dolomite
GK1-19		5004.40~5004.50	Z ₂ dn ⁴	Bitumen-bearing dolomite
GK1-22		5006.63~5006.80	Z ₂ dn ⁴	Bitumen-bearing dolomite
MX13-2		5035.05~5035.14	Z ₂ dn ⁴	Bitumen-bearing dolomite
MX13-3		5035.14~5035.36	Z ₂ dn ⁴	Bitumen-bearing dolomite
MX13-6		5045.90~5045.98	Z ₂ dn ⁴	Bitumen-bearing dolomite
MX13-11		5101.07~5101.28	Z ₂ dn ⁴	Bitumen-bearing dolomite

equivalent vitrinite reflectance (EqVR_o) of mudstone and reservoir solid bitumen are listed in Table 2. For the Lower Cretaceous mudstones (termed as lacustrine mudstones in below text), the TOC value ranges from 0.40 to 3.28%. The hydrocarbon potential (S₁ + S₂) varies from 0.96 to 18.56 mg/g. The T_{max} value ranges from 432 to 451°C. The R_o value varies from 0.68 to 0.84%. These data indicate that lacustrine mudstones are poor to good quality source rocks [28], which are at the immature to mature stages. HI versus T_{max} values show that types of organic matter are type I and type II (Figure 2). For the Lower Cambrian mudstones (termed as marine mudstones in below text), the TOC value ranges from 1.11 to 1.34%. The S₁ + S₂ value varies from 0.05 to 0.11 mg/g. The HI value ranges from 3 to 5 mg/g. The EqVR_o value is 2.63%. These data indicate that marine mudstones belong to good quality source rocks [28]. Source rocks had very high degree of thermal evolution with rare soluble extract and reached the stage of dry gas generation. The EqVR_o value of the Upper Ediacaran reservoir solid bitumen is 2.80%, indicating a very high degree of thermal evolution. Previous studies showed that type of organic matter for marine mudstones was mainly type I [38, 42].

4.2. REE Compositions of Mudstone and Corresponding Organic Fractions. REE concentrations of mudstone whole rocks and corresponding organic fractions (kerogen, extract, and reservoir solid bitumen) are presented in Table 3. REE concentrations of mudstone whole rocks normalized to the Australian Post-Archean Shale (PAAS) are shown in Figure 3. The sum of rare earth elements (ΣREE) in lacustrine mudstones ranges between 206.70 and 291.84 ppm, which is slightly higher than that in marine mudstones (166.99-233.74 ppm). The total concentration of light rare earth elements (LREE: La–Eu) in all mudstones is higher than that of heavy rare earth elements (HREE: Gd–Lu), and the LREE/HREE ratio ranges from 6.07 to 10.12. The

PAAS-normalized pattern of all mudstones shows a relatively flat pattern (Figure 3). The (La/Yb)_N ratio of mudstones varies from 0.72 to 1.10 (Table 3). The Ce/Ce* value of lacustrine mudstones ranges from 0.93 to 0.98, which is slightly higher than that of marine mudstones (0.89-0.92). The Eu/Eu* value of lacustrine mudstones ranges from 0.78 to 0.86, which is slightly lower than that of marine mudstones (0.87-0.96).

ΣREE in lacustrine kerogens ranges from 229.30 to 2282.06 ppm. The LREE/HREE ratio varies from 5.56 to 18.53. The (La/Yb)_N ratio varies from 0.65 to 2.24. The Ce/Ce* value ranges from 0.95 to 0.98. The Eu/Eu* value ranges from 0.72 to 0.87. ΣREE in marine kerogens ranges from 417.54 to 571.66 ppm. The LREE/HREE ratio varies from 18.83 to 69.01. The (La/Yb)_N ratio varies from 3.53 to 44.82. The Ce/Ce* value ranges from 0.90 to 0.98. The Eu/Eu* value ranges from 0.20 to 0.45. ΣREE in most of mudstone kerogens is higher than that in corresponding whole rocks. The degree of fractionation between LREE and HREE in marine kerogen is significantly higher than that in lacustrine kerogen. REE concentrations of kerogens normalized to corresponding whole rocks show a slight enrichment of LREE relative to HREE and no pronounced Ce and Eu anomalies in the lacustrine mudstone kerogen, but marine mudstone kerogen displays a strongly enrichment of LREE, strongly negative Eu anomalies, and no pronounced Ce anomalies (Figure 4).

The ΣREE value in lacustrine extracts ranges from 0.11 to 4.21 ppm, which is much less than that in the corresponding whole rocks and kerogens. The LREE/HREE ratio ranges from 9.46 to 15.19, indicating an enrichment of LREE. The (La/Yb)_N ratio of extracts varies from 0.62 to 2.25, which is close to that in kerogens rather than whole rocks, indicating that REE in the extract may originate directly from kerogens. The Ce/Ce* value ranges from 0.91 to 0.99, and the Eu/Eu* value ranges from 0.84 to 1.15.

TABLE 2: Bulk geochemical parameters of studied mudstone samples.

Sample No.	TOC (%)	S ₁ (mg/g)	S ₁ + S ₂ (mg/g)	HI (mg/g)	T _{max} (°C)	R _o or EqVR _o (%)
Aer3-232	3.19	0.73	18.56	559	441	n.d
Aer4-239	3.28	1.10	15.78	448	442	0.68-0.84/0.76 (6) ^a
Aer2-433	0.40	0.22	0.96	185	451	n.d
Aer11-502	1.87	0.42	13.28	688	432	n.d
GK1-1	1.11	0.03	0.09	5	478 ^c	2.62 (1) ^b
GK1-7	1.34	0.03	0.11	5	520 ^c	2.38-2.81/2.63 (4) ^b
GK1-13	1.13	0.01	0.05	3	397 ^c	n.d
GK1-18	n.d	n.d	n.d	n.d	n.d	2.53-2.95/2.80 (16) ^b

^aRange/mean (measuring points). Vitrinite reflectance (R_o). ^bReflectance of bitumen (BR_o) was converted to the EqVR_o value based on following equation: EqVR_o = 0.618 × BR_o + 0.40 [47]. ^cUnreliable T_{max} values were resulted from the lower S₂ values. n.d: not determined.

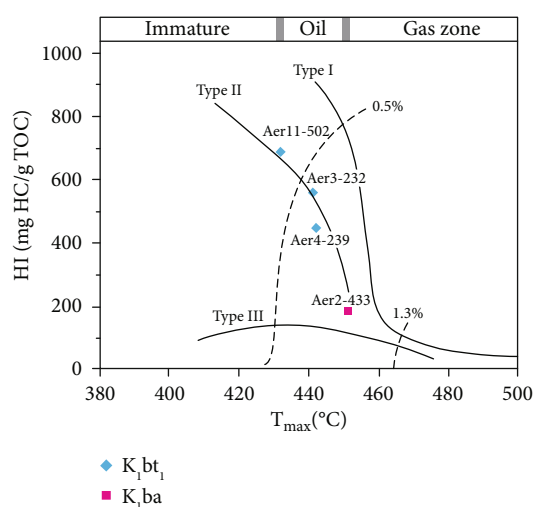


FIGURE 2: HI versus T_{max} values of mudstone samples from the Aer Sag.

The Σ REE value in the Upper Ediacaran reservoir solid bitumens ranges from 0.24 to 1.36 ppm, which is much less than that in the lower Cambrian mudstones and corresponding kerogens. The LREE/HREE ratio ranges from 9.53 to 24.60, indicating an enrichment of LREE. The PAAS-normalized REE pattern shows a slight enrichment of LREE (Figure 5). The highly similarities of REE patterns in reservoir solid bitumens suggest the same origin. The Ce/Ce* value ranges from 0.78 to 0.96. Notably, reservoir solid bitumens display strongly positive Eu anomalies (Eu/Eu* = 8.17 – 150.54).

4.3. Trace Element Compositions of Mudstone and Corresponding Organic Fractions. Trace element concentrations of whole rock and corresponding organic fractions (kerogen, extract, and reservoir solid bitumen) are presented in Table 4. The PAAS-normalized trace element pattern of mudstone whole rocks is shown in Figure 6 [46, 48]. Some trace elements (e.g., Cs, U, Mo, and REE) are enriched in lacustrine mudstones while other elements (e.g., Sr, Ni, and Cr) are depleted relative to PAAS. A similar pattern in lacustrine mudstones suggests they have a same provenance (Figure 6).

Majority of trace elements are enriched in marine mudstones. Especially, U and Mo are highly enriched, whereas Sr is depleted (Figure 6). A highly similar pattern in marine mudstones indicates that they have not only a same provenance but also a relatively stable depositional environment.

Concentrations of trace elements in the isolated organic fractions were normalized to corresponding whole rock and plotted in Figure 7. Lithophile elements (e.g., Cs, Rb, and Ba) and V are depleted in lacustrine kerogens relative to whole rocks, while REE and Ni are enriched. The trace element pattern of lacustrine kerogens largely varies, which might be related with the organic matter in lake under an unstable paleoredox environment. Lithophile elements, Sc, and V are depleted in marine kerogens relative to whole rocks, while LREE, Mo, Co, Ni, and Cu are enriched. The trace element pattern of marine kerogens shows little changes, which might be closely related with relatively stable paleoredox environment of the early Cambrian ocean. All trace elements are depleted in lacustrine extracts relative to whole rocks, while only Ni is relatively enriched in the individual sample (Figure 7). Overall, the concentration of transition metal elements (V, Cr, Co, Ni, Cu, and Zn) and redox-sensitive metal elements (U and Mo) is higher than the rest elements in lacustrine extracts.

The PAAS-normalized trace element pattern of the upper Ediacaran reservoir solid bitumens shows that majority of trace elements are depleted (Figure 8), while Mo, V, Ni, and Pb are enriched relative to the rest elements. Especially, Mo is highly enriched. A similar pattern of reservoir solid bitumens indicates they share the same origin.

5. Discussion

5.1. Depositional Environment of Mudstones. Jones and Manning found that the parameters of U/Th, authigenic U, V/Cr, and Ni/Co were the reliable geochemical indices for the interpretation of paleoredox conditions in ancient mudstones [7]. In this study, U/Th ratios show that lacustrine mudstones deposited under oxic to dysoxic conditions while marine mudstones deposited under anoxic conditions (Figure 9). The authigenic U of lacustrine mudstones ranges from -0.40 to 14.27, showing that most of mudstones deposited in oxic conditions while individual mudstone deposited

TABLE 3: Rare earth element concentrations (ppm) and associated parameters of whole rock, kerogen, extract, and reservoir solid bitumen samples.

	La	Ce	Pr	Nd	Sm	Eu	Gd	Tb	Dy	Ho	Er	Tm	Yb	Lu	Σ REE	LREE/HREE	(La/Yb) _N	Ce/Ce*	Eu/Eu*
Whole rock																			
Aer3-232	52.7	103	12.5	47.7	9.61	1.53	8.79	1.66	9.53	1.84	5.36	0.889	5.39	0.847	261.35	6.62	0.72	0.93	0.78
Aer4-239	58.7	121	14.4	54	10.6	1.68	9.14	1.56	8.45	1.54	4.65	0.736	4.67	0.714	291.84	8.28	0.93	0.96	0.80
Aer2-433	41.9	85.1	10.1	38.8	7.29	1.21	6.02	1.05	5.83	1.12	3.4	0.594	3.68	0.601	206.70	8.27	0.84	0.95	0.86
Aer11-502	57.1	117	13.3	49.3	8.63	1.29	7.03	1.17	6.35	1.19	3.61	0.591	3.82	0.615	271.00	10.12	1.10	0.98	0.78
GK1-1	43.5	85.5	11.4	46.5	11.6	2.19	10.6	1.87	9.33	1.67	4.46	0.636	3.93	0.553	233.74	6.07	0.82	0.89	0.93
GK1-7	40.1	74.9	8.84	30.3	5.26	0.99	4.49	0.815	4.6	0.941	2.8	0.456	2.95	0.443	177.89	9.17	1.00	0.92	0.96
GK1-13	40	70.9	8.12	27.7	4.11	0.718	3.7	0.684	3.86	0.813	2.56	0.432	2.96	0.435	166.99	9.81	1.00	0.91	0.87
Kerogen																			
Aer3-232	45.6	91.3	10.4	38.6	7.21	1.21	7.89	1.66	10.7	2.01	5.89	0.907	5.18	0.743	229.30	5.56	0.65	0.97	0.76
Aer4-239	63.4	127	14	50.4	8.44	1.27	7.53	1.41	8.57	1.67	4.73	0.692	3.61	0.489	293.21	9.22	1.30	0.98	0.75
Aer2-433	523	1041	117	414	61.1	9.13	39.6	5.58	28.2	5.15	15.7	2.64	17.2	2.76	2282.06	18.53	2.24	0.97	0.87
Aer11-502	163	284	29.2	97.9	14	1.9	10.9	1.84	11	2.23	7.23	1.23	7.96	1.27	633.66	13.51	1.51	0.95	0.72
GK1-1	109	191	21.4	69	5.43	0.65	8.51	1.09	4.31	0.951	3.21	0.412	2.28	0.298	417.54	18.83	3.53	0.91	0.45
GK1-7	158	265	28.9	92.9	7.07	0.566	10.7	1.07	2.59	0.572	2.48	0.246	1.39	0.177	571.66	28.74	8.39	0.90	0.31
GK1-13	221	247	15.4	27.8	0.852	0.096	5.73	0.305	0.31	0.073	0.541	0.051	0.364	0.047	519.57	69.01	44.82	0.98	0.20
Extract																			
Aer3-232	0.272	0.543	0.059	0.23	0.043	0.007	0.036	0.006	0.036	0.006	0.019	0.003	0.014	0.002	1.28	9.46	1.43	0.99	0.84
Aer4-239	0.025	0.048	0.005	0.017	0.004	n.d	0.002	n.d	0.004	n.d	n.d	n.d	0.003	n.d	0.11	11.00	0.62	0.99	—
Aer2-433	0.262	0.534	0.07	0.293	0.063	0.013	0.045	0.008	0.028	0.006	0.012	n.d	0.011	n.d	1.35	11.23	1.76	0.91	1.15
Aer11-502	0.932	1.86	0.214	0.787	0.136	0.021	0.095	0.015	0.071	0.012	0.032	0.005	0.027	0.003	4.21	15.19	2.55	0.96	0.87
Reservoir solid bitumen																			
GK1-18	0.065	0.127	0.018	0.068	0.014	0.121	0.011	n.d	0.007	n.d	0.005	n.d	0.004	n.d	0.44	15.30	1.20	0.86	45.91
GK1-19	0.165	0.218	0.025	0.123	0.026	0.747	0.021	n.d	0.009	n.d	0.017	n.d	0.006	n.d	1.36	24.60	2.03	0.78	150.54
GK1-22	0.057	0.098	0.011	0.046	0.007	0.016	0.007	n.d	0.006	n.d	0.004	n.d	0.003	n.d	0.26	11.75	1.40	0.90	10.76
MX13-2	0.103	0.146	0.018	0.072	0.011	0.082	0.011	n.d	0.012	n.d	0.005	n.d	0.005	n.d	0.47	13.09	1.52	0.78	35.10
MX13-3	0.054	0.077	0.009	0.042	0.01	0.136	0.008	n.d	0.006	n.d	0.004	n.d	0.003	n.d	0.35	15.62	1.33	0.81	71.60
MX13-6	0.092	0.123	0.014	0.064	0.012	0.019	0.01	n.d	0.012	n.d	0.006	n.d	0.006	n.d	0.36	9.53	1.13	0.79	8.17
MX13-11	0.042	0.081	0.009	0.045	0.01	0.033	0.006	n.d	0.006	n.d	0.004	n.d	0.003	n.d	0.24	11.58	1.03	0.96	20.06
GK1-18	0.065	0.127	0.018	0.068	0.014	0.121	0.011	n.d	0.007	n.d	0.005	n.d	0.004	n.d	0.44	15.30	1.20	0.86	45.91

LREE/HREE = (La + Ce + Pr + Nd + Sm + Eu)/(Gd + Tb + Dy + Ho + Er + Tm + Yb + Lu). n.d: the concentration of element is less than 0.002 ppm and below the limit of detection. -: no available data.

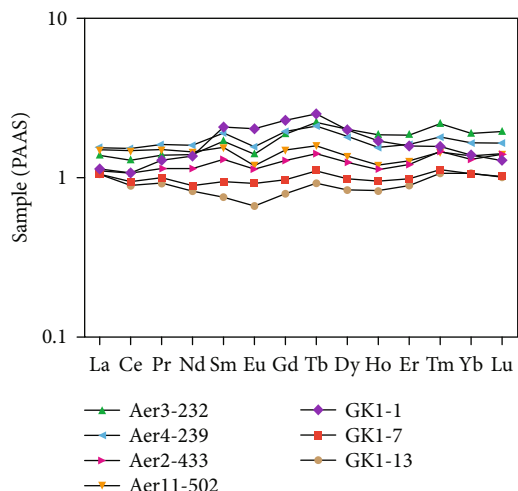


FIGURE 3: PAAS-normalized plots of rare earth elements in whole rock samples (PAAS from [46]).

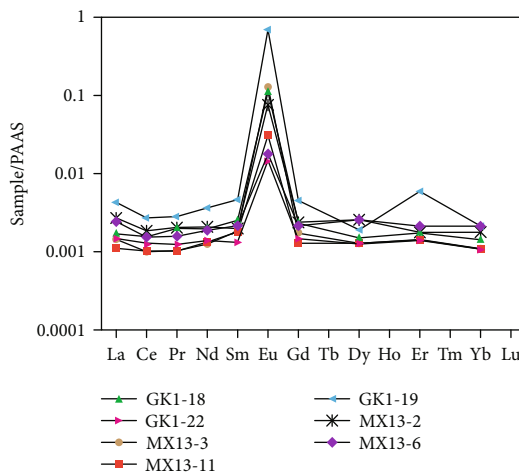


FIGURE 5: PAAS-normalized plot of the rare earth elements in the Upper Ediacaran reservoir solid bitumens (PAAS from [46]).

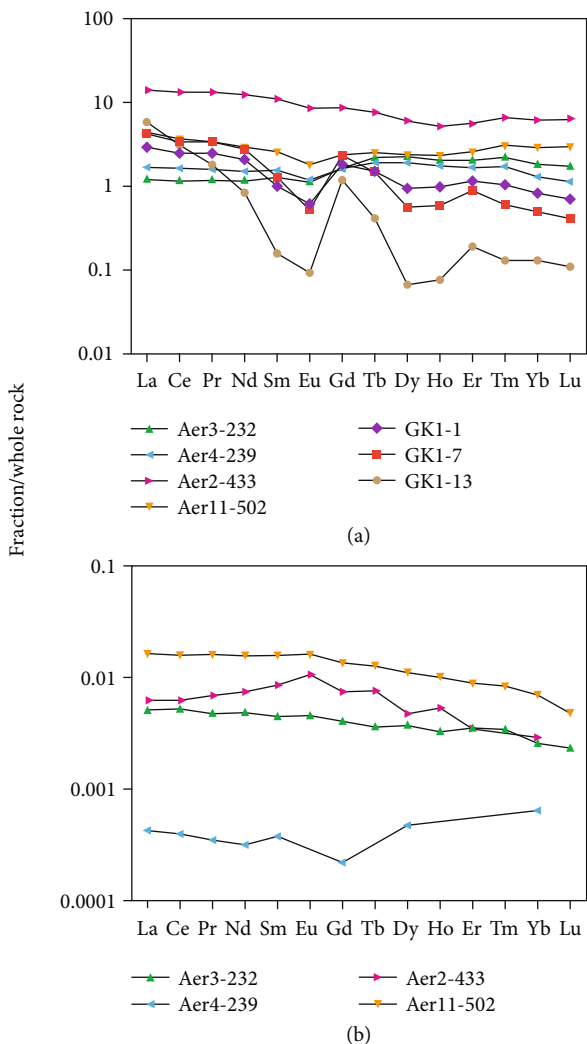


FIGURE 4: REE concentrations of isolated organic fractions ((a) kerogen and (b) extract fractions)) of mudstones normalized to corresponding whole rock.

in anoxic condition. The authigenic U of marine mudstones ranges from 11.63 to 44.33, showing an anoxic depositional environment. The V/Cr ratios of lacustrine and marine mudstones are less than 2.00, representing an oxic depositional environment. This interpretation is not consistent with the depositional environment defined by above two parameters. Abanda and Hannigan suggested that V/Cr ratios below 2 might reflect a diagenetic overprint [1]. Ni/Co ratios less than 5.00 are representative of deposition under oxic conditions [7]. Our data suggests that lacustrine mudstones deposited in oxic conditions. The Ni/Co ratio of marine mudstones ranges from 3.40 to 5.67, showing oxic to dysoxic depositional environments. However, Abanda and Hannigan observed that Ni/Co ratios of mudstones decreased with increasing maturity [7].

Recent studies show that majority of the Lower Cretaceous mudstones in Erlian Basin preferred to an oxic depositional environment and only few mudstones deposited in the weakly reducing environments [49]. The early Cambrian in South China was in the periods of largest marine transgression and “biological explosion” around the world [3–5, 14]. A succession of black organic-rich shales and mudstones of early Cambrian age was developed widely throughout South China. It has been considered anoxic sediments [3–5, 14] and one of most important source rocks in Sichuan Basin [44]. Laminated pyrites were often observed in the Lower Cambrian black mudstones from core description, indicating that mudstones should be deposited under anoxic conditions. Consequently, a wrong conclusion may be drawn during the identification of depositional environments in mudstones using single trace element parameter. Tribouvillard et al. suggested that detrital, hydrothermal, and biogenic materials in sediments and sedimentary rocks (that is, nonauthigenic components) must be excluded when we used trace element concentrations and/or ratios to reconstruct paleoenvironmental conditions [13]. For example, authigenic U is a better proxy to reconstruct the depositional environment of mudstones in this study. Additionally, kerogen in mudstones can be regarded as a special kind of authigenic component [14] and therefore trace and rare earth

TABLE 4: Trace element concentrations (ppm) and associated parameters of whole rock, kerogen, extract, and reservoir solid bitumen samples.

	Cs	Rb	Ba	Th	U	Pb	Mo	Sr	Y	Sc	V	Cr	Co	Ni	Cu	Zn	U/Th	Auth U	V/Cr	Ni/co	V/Ni
Whole rock																					
Aer3-232	101	255	550	27.6	10.2	44.1	5.81	110	53.2	17	115	71	14	28.3	49.7	148	0.37	1.00	1.62	2.02	4.06
Aer4-239	108	195	559	23.5	22.1	40.6	28.7	138	45.9	14	82.5	77.4	18.1	38.3	39.6	140	0.94	14.27	1.07	2.12	2.15
Aer2-433	56.6	151	606	14.9	4.57	30.5	1.48	167	32.3	12.3	72.3	46.5	12.2	21.2	27.1	93.9	0.31	-0.40	1.55	1.74	3.41
Aer11-502	74.5	206	475	22.3	10.5	56	19.5	188	34.2	11.6	78.1	45.1	19.9	23.2	25.6	238	0.47	3.07	1.73	1.17	3.37
GK1-1	6.48	119	740	12.2	48.4	62	49.9	113	48.8	21	194	99.7	16.4	93	44.8	191	3.97	44.33	1.95	5.67	2.09
GK1-7	5.52	104	695	11.1	19.2	63.4	26.9	111	26.8	14.1	159	85.8	17.9	67.5	49.7	44.5	1.73	15.50	1.85	3.77	2.36
GK1-13	6.12	110	716	10.7	15.2	80.7	23.5	98.9	23.1	15.1	163	92.3	17.6	59.8	50.6	35.7	1.42	11.63	1.77	3.40	2.73
Kerogen																					
Aer3-232	42.2	98.2	126	16.5	3.83	28.4	1.03	28.6	65.7	3.53	6.68	12.9	6.12	39	24.6	47.3	0.23	-1.67	0.52	6.37	0.17
Aer4-239	1.57	3.32	21.8	11.9	4.96	2.66	6.6	33.7	52.8	0.536	2.02	22.6	6.32	75.8	18.9	61.1	0.42	0.99	0.09	11.99	0.03
Aer2-433	24.6	78	288	54.9	13.5	24.3	2.04	217	148	21.8	25.7	118	27.1	114	177	80	0.25	-4.80	0.22	4.21	0.23
Aer11-502	22.1	424	370	28	8.82	6.55	7.59	174	69.3	13.5	13.3	23	16	34.4	24.8	74.4	0.32	-0.51	0.58	2.15	0.39
GK1-1	0.029	0.352	19.6	8.67	13.5	291	151	117	28.6	2.45	28.6	38.3	102	606	419	67.7	1.56	10.61	0.75	5.94	0.05
GK1-7	0.04	0.323	24.3	10.8	9.78	501	438	168	16.8	1.58	25.1	57.2	141	682	510	99.9	0.91	6.18	0.44	4.84	0.04
GK1-13	0.052	0.614	12.4	3.92	12.4	633	175	119	2.61	0.369	73.5	128	74.2	851	528	21.3	3.16	11.09	0.57	11.47	0.09
Extract																					
Aer3-232	0.598	1.44	5.92	0.12	0.118	1.43	0.248	0.925	0.21	0.108	3.89	2.18	0.966	32.3	3.95	8.87	0.98	0.08	1.78	33.44	0.12
Aer4-239	0.017	0.071	1.44	0.01	0.04	0.372	0.568	0.374	0.018	0.017	2.97	2.85	0.394	23.4	3.45	8	4.00	0.04	1.04	59.39	0.13
Aer2-433	0.606	1.25	8.94	0.074	0.208	1.27	0.22	2.39	0.13	0.139	1.54	3.58	0.759	5.78	10.8	21.9	2.81	0.18	0.43	7.62	0.27
Aer11-502	1.45	2.97	13	0.327	0.379	2.16	2.23	3.29	0.362	0.23	14.3	4.47	33.1	229	16.3	61.9	1.16	0.27	3.20	6.92	0.06
Reservoir solid bitumen																					
GK1-18	0.015	0.495	203	0.043	0.032	17.6	19	1.69	0.037	0.146	262	0.975	0.192	126	2.2	4.64	0.74	0.02	268.72	656.25	2.08
GK1-19	0.021	0.361	971	0.043	0.038	24	28.3	5.18	0.056	0.179	197	1.42	0.389	132	1.73	5.42	0.88	0.02	138.73	339.33	1.49
GK1-22	0.01	0.289	22.8	0.024	0.068	19	46.9	1.25	0.032	0.15	577	4.31	0.368	190	5.38	3.69	2.83	0.06	133.87	516.30	3.04
MX13-2	0.017	0.278	125	0.038	0.742	26.8	90.2	4.1	0.105	0.176	420	2	0.446	225	1.41	3.22	19.53	0.73	210.00	504.30	1.87
MX13-3	0.02	0.794	231	0.016	0.025	36.8	14.8	3.85	0.03	0.154	199	3.43	0.131	139	1.26	4.66	1.56	0.02	58.02	1061.07	1.43
MX13-6	0.025	0.858	37.9	0.019	0.075	26.6	15.6	6.89	0.06	0.267	255	3.91	0.192	155	51.1	28.8	3.95	0.07	65.22	807.29	1.65
MX13-11	0.015	0.224	53.4	0.014	0.018	29.9	33.2	1.43	0.037	0.135	254	0.868	0.171	144	1.04	2.68	1.29	0.01	292.63	842.11	1.76

Auth U = (total U) - Th/3.

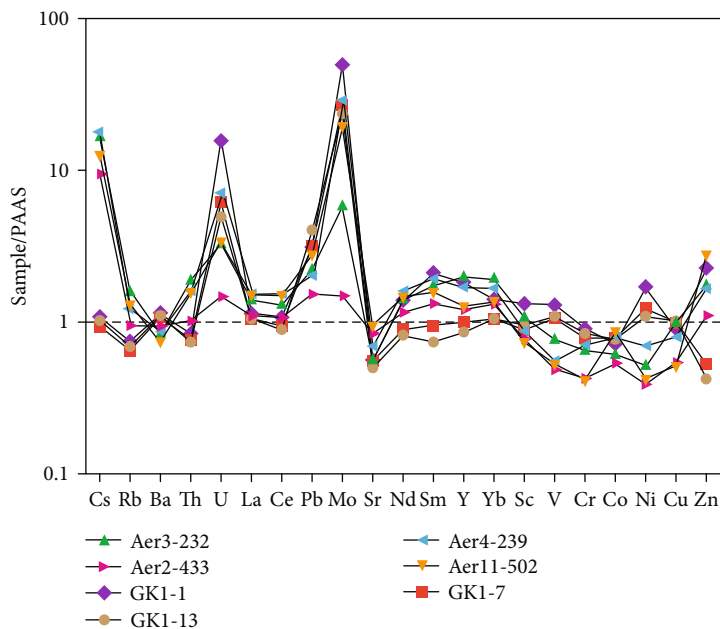


FIGURE 6: PAAS-normalized plot of trace elements in mudstones (PAAS from [46, 48]).

element compositions in kerogen may be helpful to explore paleoredox conditions of lakes and oceans. In this study, trace element ratios (e.g., Ni/Co, V/Cr, and V/Ni) show little variation in mudstone whole rocks, but they greatly changed in mudstone kerogens (Figure 10). Since redox-sensitive trace elements are more easily captured by organic matter in the reducing water columns, trace element compositions in kerogens can reflect the subtle variations of paleoredox environments during the sedimentation and early diagenesis of organic matter. Slight differences of Ce anomaly values occur between mudstone whole rocks and kerogens, whereas wide variations of Eu anomaly values are observed between them. Eu anomalies in kerogens are more depleted than that in corresponding whole rocks, especially marine kerogens (Figure 10). The strongly negative Eu anomalies in kerogens might be representative of reducing environments during the sedimentation and early diagenesis of organic matter. Nevertheless, there is still a need for robust datasets and further studies to reconstruct paleodepositional environments using trace and rare earth element concentrations and/or ratios of kerogens.

5.2. REE Partitioning between Whole Rock and Isolated Organic Fractions of Mudstones. REE concentrations of the isolated organic fractions of mudstones (kerogen and extract) were normalized to corresponding whole rocks and plotted in Figure 4. Lacustrine kerogens are slightly enriched in the LREE relative to HREE, whereas marine kerogens are strongly enriched in LREE (Figure 4). In contrast, coal and its organic fraction displayed HREE-enriched pattern [50, 51]. Such different REE patterns should be attributed to various depositional environments of organic matters. Lacustrine extracts also show a slight enrichment of LREE similar to corresponding kerogen fractions (Figure 4), suggesting that the REE pattern in extract

fractions inherited from kerogen fractions. It is well known that trace elements in crude oils were mainly found in the asphaltene fractions [20, 26–28]. Since the asphaltenes are kerogen fragments [51, 52], REE of crude oils should be mainly originated from kerogens, and the REE pattern of extracts is similar to that of kerogens (Figure 4).

REE concentrations of mudstone extracts were normalized to corresponding kerogens and plotted in Figure 11, making us understand the REE partitioning during the oil generation of kerogens. Middle rare earth elements (MREE: Sm–Ho) are enriched in extracts relative to kerogens, suggesting that MREE migrate from kerogen to extract more easily than the rest REE. Felitsyn and Morad [53] also found that the humic acid displayed a MREE enrichment. Wong et al. [54] and Radzki et al. [55] suggested that a certain portion of REE (mainly MREE) could be chelated by porphyrin complexes. This statement seems to be able to explain the MREE enrichment in extracts. In addition, significant positive Eu anomalies are observed (Figure 11). Eu is a diagnostic multivalent rare earth element, which is as stable as Eu^{3+} under the alkaline and oxidizing conditions, but Eu^{3+} can be transformed into Eu^{2+} under the acidic and reducing conditions [56]. Kerogens can generate organic acids during the oil generation. The acidic condition can be developed by the lowering pH value, and then it activates the REE. Eu^{3+} can be reduced to Eu^{2+} under the reducing environments formed by oil generation, and it then shifts into the soluble organic matters (extracts), resulting in the higher concentrations of Eu relative to the neighboring REEs (Sm and Gd) and the pronounced positive Eu anomalies.

Interestingly, the Upper Ediacaran reservoir solid bitumens display much stronger positive Eu anomalies. Eu anomalies have been reported in various types of igneous and sedimentary rocks [57]. However, reduction of Eu does not seem to occur within the ocean basins except in

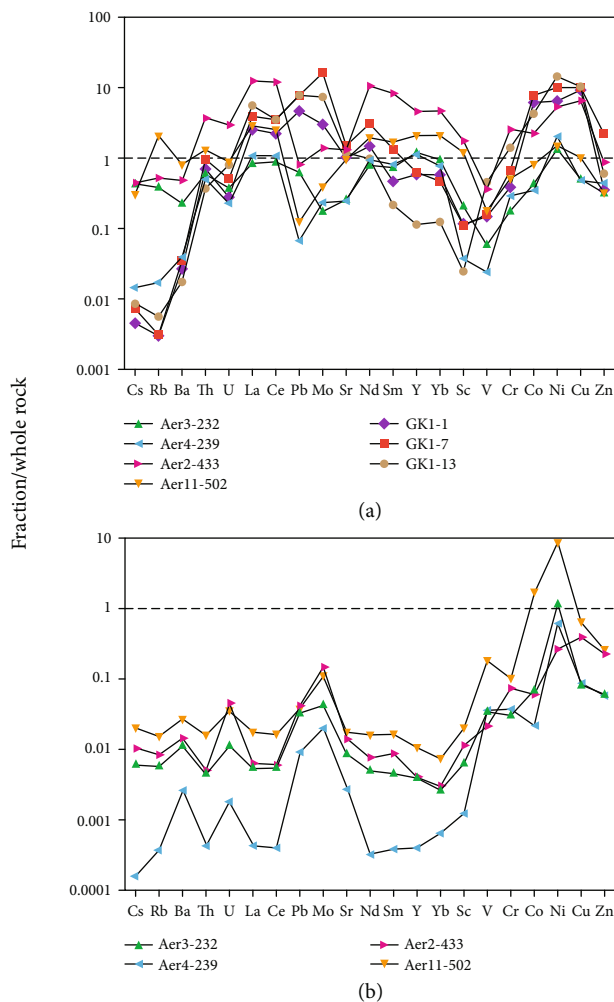


FIGURE 7: Trace elements concentrations in isolated organic fractions ((a) kerogen and (b) extract fractions) of mudstones normalized to corresponding whole rock.

submarine hydrothermal systems and during some extreme marine diagenesis in certain organic-rich, sulfate reducing environments [8, 58]. Consequently, positive Eu anomalies have been commonly found in reducing hydrothermal fluids, calcium-rich, and early magmatic minerals (e.g., plagioclase and K-feldspar) [59]. Previous authors have revealed that the Upper Ediacaran reservoir solid bitumen contains no feldspar minerals based on XRD pattern [21]; hence, the interference of feldspar minerals can be excluded. In addition, Eu^{2+} might be replaced by Sr^{2+} because the ionic radius of Eu^{2+} is close to Sr^{2+} [60], resulting positive Eu anomalies. Dulski [61] considered that positive Eu anomalies might be an artifact caused by Ba interference during ICP-MS measurement. Eu anomalies in the Upper Ediacaran reservoir bitumens show an excellent positive correlation with the concentrations of Ba (Figure 12(a)) but show a poor correlation with the concentrations of Sr (Figure 12(b)), suggesting that Eu anomalies in reservoir solid bitumens may be a result of Ba interference. Eu anomalies in the Cambrian reservoir bitumens from Sichuan Basin had also been reported [62]. They were interpreted

as the inheritance of the Lower Cambrian black shales, since the formation of this unit of black shales and the development of polymetallic beds were considered related with submarine hydrothermal venting [14, 63]. However, there is no clear evidence indicating that the Lower Cambrian black mudstones in the Central Sichuan Basin have a hydrothermal origin, such as no positive Eu anomalies in mudstones from this study. Consequently, strongly positive Eu anomalies in reservoir solid bitumens may be a result of Ba interference. If Ba interference is not taken into consideration, we prefer to believe that Eu mobilization is caused by the strongly reducing microenvironment formed by thermal degradation of kerogen.

5.3. Trace Element Partitioning between Whole Rock and Isolated Organic Fractions of Mudstones. Redox-sensitive trace elements (e.g., U, Mo, and Ni) and REE are enriched in both lacustrine and marine kerogens relative to whole rocks, while lithophile elements (e.g., Cs, Rb, Ba, and Sc) are depleted (Figure 7). Th is generally considered to concentrate in the clastic components, which is an immobile element [64]. However, Th is enriched in kerogen relative to whole rock. This may be related with an enrichment of elements associated with dense refractory heavy minerals caused by gravity settling during the isolation of kerogen (e.g., Zr) [1]. The elements U, Ni, and V generally tend to associate with organic matter in black shales [65]. However, compared with other elements, V in both lacustrine and marine kerogens shows depletion relative to whole rocks. Especially, V is strongly depleted in lacustrine kerogens (Figure 7), which may be related with its geochemical behavior under various redox environments and occurrence state in sediments (see below text for detailed discussion). These redox-sensitive metal elements were easily adsorbed by organic matter and/or captured by porphyrin complexes during the settlement processes of organic particles; thus, they are relatively enriched in kerogens.

The concentrations of trace elements in lacustrine extracts were normalized to corresponding kerogens and plotted in Figure 13. Compared with other trace elements, REE is still not easy to remove from kerogen to soluble hydrocarbons, which may be related with a lack of appropriate chelating sites in the soluble hydrocarbons during primary migration [25]. An obvious trend is that transition metal elements (e.g., Mo, V, Cr, Co, Ni, Cu, and Zn) released from kerogen to soluble hydrocarbons more easily than the rest elements, especially V and Ni (Figure 13). Ni in lacustrine extracts has the highest concentrations. Compared with Ni, the lower concentrations of V seem to be related with weak oxidizing depositional environments of lacustrine mudstones. During thermal maturation of organic matter, a large amount of oxygen-containing and sulfur-containing functional groups will be released from kerogens, which play a significant role in the removal of trace elements. For example, carboxyl and phenolic hydroxyl groups can provide complexing sites for Ca^{2+} , REE, and other elements [66, 67].

5.4. The Enrichment and Mobilization of Trace Elements in Organic Fractions of Mudstones. Compared with other trace

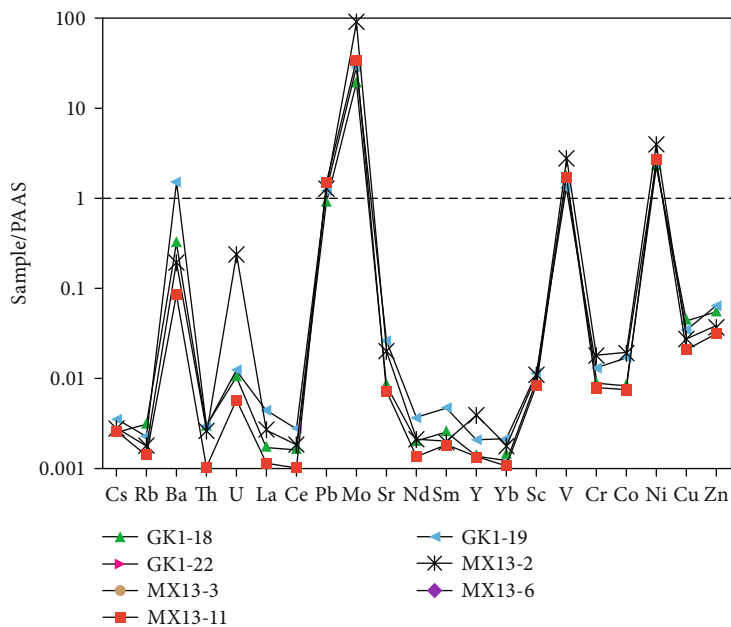


FIGURE 8: The PAAS-normalized plot of trace elements in the upper Ediacaran reservoir solid bitumens (PAAS from [48]).

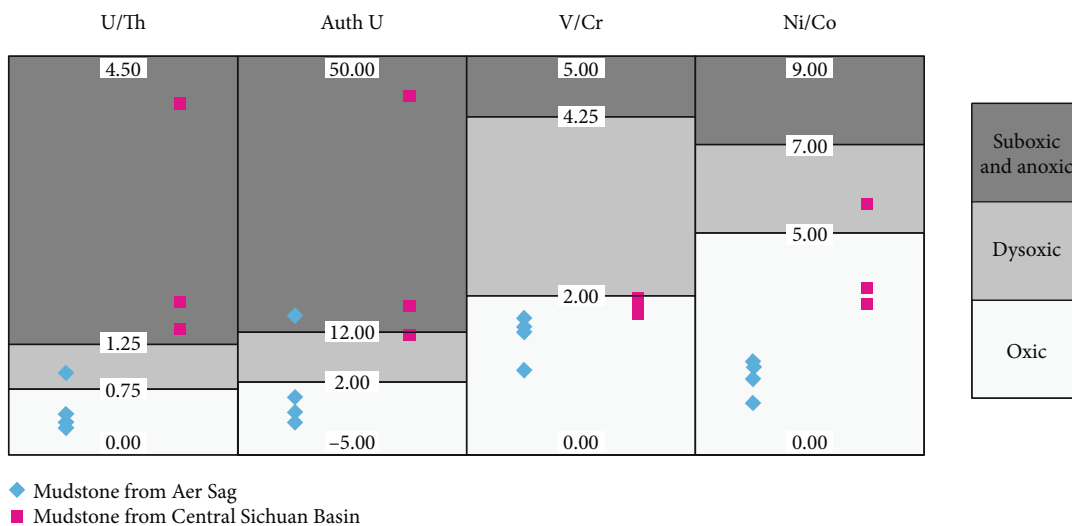


FIGURE 9: The identification of depositional environment of mudstones using trace element parameters (criteria of redox environments from [7]).

elements, some elements such as U, Mo, Ni, and Cu are enriched in both lacustrine and marine kerogens relative to whole rocks, while V is depleted (Figure 7). In the lacustrine extracts, Ni has the highest concentration, and U, Mo, and V are relatively enriched (Figure 7). Compared with other elements, Mo is strongly enriched in the Upper Ediacaran reservoir solid bitumens, and V, Ni, Pb, U, and Ba are relatively enriched (Figure 8). The enrichment of these elements is closely related with their geochemical behaviors in the various depositional and diagenetic environments.

- (1) *Mo*. Mo is present mainly in the form of molybdate (MoO_4^{2-}) [68]. Mo is not concentrated by ordinary plankton nor is it readily adsorbed by most types of natural particles, and it displays little affinity for

the surfaces of clay minerals, CaCO_3 , and Fe-oxhydroxides under the weakly alkaline marine conditions [69]. By contrast, Mo is easily captured by the surface of Mn-oxhydroxides [70]. MoO_4^{2-} cannot directly react with H_2S to form MoS_2 or MoS_3 under the reducing condition, but instead, it is precipitated in the form of thiomolybdates ($\text{Mo}(\text{O}_x, \text{S}_{4-x})^{2-}$ ($x = 0 \sim 3$)) and inorganic Fe-Mo-S cluster complexes possibly occurring in Fe-sulfides through the incorporation of organic matter [71]. Organic O-S groups attached to macromolecular detritus may insert directly into the MoO_4^{2-} , resulting in covalent bonding between Mo and the macromolecular, and then Mo will be scavenged from water columns [13]. Consequently, the Mo content

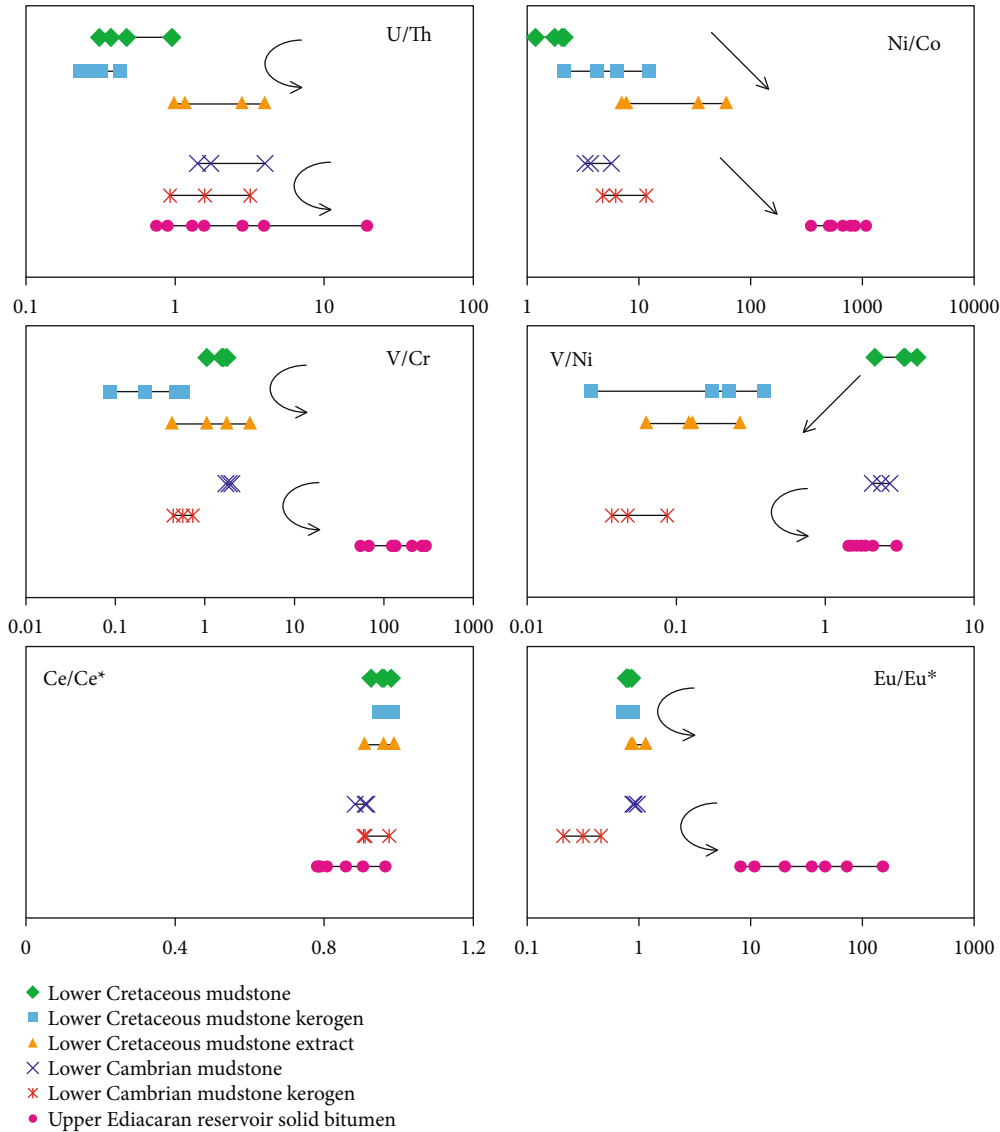


FIGURE 10: Diagram showing the comparison of redox-sensitive trace element ratios and REE parameters in the whole rock, kerogen, and extract/reservoir solid bitumen. Trace element ratios (e.g., Ni/Co, V/Cr, and V/Ni) show little variation in mudstone whole rocks, but they greatly changed in mudstone kerogens, reflecting the subtle variations of paleoredox environments during the sedimentation and early diagenesis of organic matter. U/Th, V/Cr, and V/Ni ratios show a decreasing trend between mudstone whole rock and kerogen, indicating that U and V may occur more in mineral phases of mudstone. Ni/Co ratios show an increasing trend between mudstone whole rock and kerogen, indicating that Ni may occur more in organic phases of mudstones. U/Th, Ni/Co, and V/Cr ratios display an increasing trend between mudstone kerogen and extract/reservoir bitumen, suggesting that redox-sensitive trace elements (U, Ni, and V) may be released from kerogens more easily than other elements. Slight differences of Ce anomaly values occur among mudstone whole rock, kerogen, and extract/reservoir bitumen, whereas Eu anomalies in kerogens are more depleted than that in corresponding whole rocks, especially marine kerogens. The strongly negative Eu anomalies in kerogens might be representative of reducing environments during the sedimentation and early diagenesis of organic matter.

of sediments is closely related to the S content, which increases with the enhanced anoxic conditions [13]. During the thermal degradation of organic matter, Mo inevitably moved into crude oils with the release of sulfur-containing functional groups. The XRD pattern of Ediacaran reservoir solid bitumen shows that a large amount of sulfur-containing compounds and elemental sulfur occurred in bitumens [22]. They provide substantial coordination bonds for

Mo, resulting that Mo is strongly enriched in reservoir solid bitumens. As a result, the enrichment degree of Mo in expelled hydrocarbons depends on the differences of Mo content in mudstones

- (2) V. In oxic waters, V is present generally in the form of vanadate oxyanions (HVO_4^{2-} and H_2VO_4^-). Vanadate readily adsorbs onto both Mn- and Fe-oxyhydroxides [72] and possibly kaolinite [73]. Under mildly

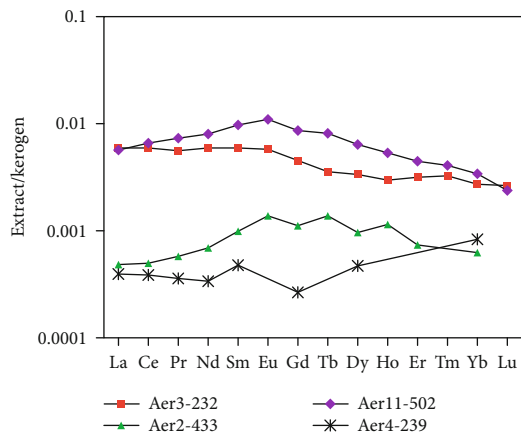


FIGURE 11: Rare earth elements in extract fraction of mudstones normalized to corresponding kerogen fraction.

reducing conditions, V^{5+} is reduced to V^{4+} and forms vanadyl ions (VO^{2+}), related hydroxyl species ($VO(OH)_3^-$), and insoluble hydroxides ($VO(OH)_2$). This reaction is favored by the presence of humic and fulvic acids. The V^{4+} ionic species may be removed to sediment by surface adsorption processes or by formation of organometallic ligands [9]. Under more strongly reducing (or sulfidic) conditions, V will be further reduced to V^{3+} which can be taken up by geoporphyryns or be precipitated as the solid oxide V_2O_3 or hydroxide $V(OH)_3$ phase [13]. Consequently, various redox environments control not only the total content of V in sediments but also the content of V in sedimentary organic matters (termed as organic V). In this study, the depletion degree of V in lacustrine kerogen relative to whole rock is higher than that in marine kerogen (Figure 7), indicating that the enrichment degree of organic V in sediments is different under various redox environments. During the oil generation of kerogen, porphyrin complexes can provide suitable coordination sites for removal of V. Since heavy oils showed good correlation between the sulfur content and the V concentration, Tissot and Welte [26] suggested that V was mainly bound to chemical structures containing sulfur. The V enrichment of the Upper Ediacaran reservoir solid bitumens indicates that their source rocks had a high proportion of organic V and deposited in the strongly reducing (or sulfidic) environments (Figure 8).

- (3) *Ni*. Different from V, Ni is a micronutrient element [13]. It is mainly associated with organic matters and then transported to sediments. In oxic conditions, Ni is mostly present as a soluble carbonate ($NiCO_3$) or adsorbed onto humic and fulvic acids [2, 70]. But complexation of Ni with organic matter will accelerate scavenging in the water column and thus sediment enrichment [74]. Under reducing (sulfidic) conditions, Ni may be incorporated as the insoluble NiS into pyrite [13]. Occasionally, the Ni brought to the sedi-

ments by organic matters may also be incorporated into tetrapyrrole complexes and may be preserved as Ni geoporphyryns under reducing conditions [75]. In this study, Ni is enriched in both lacustrine and marine kerogens relative to whole rock (Figure 7), indicating that Ni is more concentrated in the organic phase of mudstone. Nonetheless, the concentration of V is still larger than Ni in the Upper Ediacaran reservoir solid bitumens ($V/Ni = 1.43 - 3.04$), which is consistent with the result of $V/Ni > 1$ in marine oils [19]. There are two reasons leading to this result: (a) V porphyrin complex has the greater stability than Ni porphyrin complex, and VO^{5+} can replace the Ni^{2+} [76]; (b) V can be bound to sulfur-containing compounds and thus released from kerogen

- (4) *U*. In reducing conditions, dissolved U^{6+} is reduced to U^{4+} , and it is precipitated in the form of uraninite (UO_2 , U_3O_7 , or U_3O_8) or hydroxyl complexes with greater surface activity and thus enriched in sediments [77, 78]. The removal of U from the water column to the sediments may be accelerated by the formation of organometallic ligands in humic acids [13, 77, 78], the U uptake by organic substrates in sediments [2], and bacterial sulfate reduction reactions [77, 78], and thus, U enrichment in sediments is enhanced. Under strongly reducing (or sulfidic) conditions, U concentration shows a weak correlation with the organic carbon content, indicating that U is mainly occurred in authigenic mineral phases rather than organic phases [2, 13]. Therefore, U is strongly enriched in mudstones, but it is not strongly enriched in organic matter of mudstones (kerogen, extract, and reservoir bitumen; Figures 6–8)
- (5) *Ba*. Ba is present in sediments mainly in the form of barite ($BaSO_4$) [13, 79]. In surface water, live phytoplankton actively or passively incorporates Ba and Ba released during phytoplanktonic necromass decay may precipitate as barite in microenvironments (e.g., organic matter-rich particles, foram chambers, and fecal pellets) [79]. Consequently, the concentration of biogenic Ba and the abundance of barite have long been used as proxies for paleoproductivity [3, 12, 79]. Decay of organic matter will release biobarite, and the mobility of Ba during anoxic diagenesis appears quite large [6, 59]. The high concentration of Ba in the Upper Ediacaran solid bitumens (Figure 8) suggests that their source rocks may have a higher abundance of barite. Previous studies showed that the lowermost Cambrian black shales in South China hosted the world's largest barite deposits [80]. Bioaccumulation of barite from upwelling of nutrient-rich waters has been proposed for the formation of these deposits [81]. Recent drilling results show that an intraplateform basin was formed in Central-Southern Sichuan Basin [5, 43, 44, 82]. The natural gas and reservoir solid bitumen from the Upper Ediacaran dolomites are

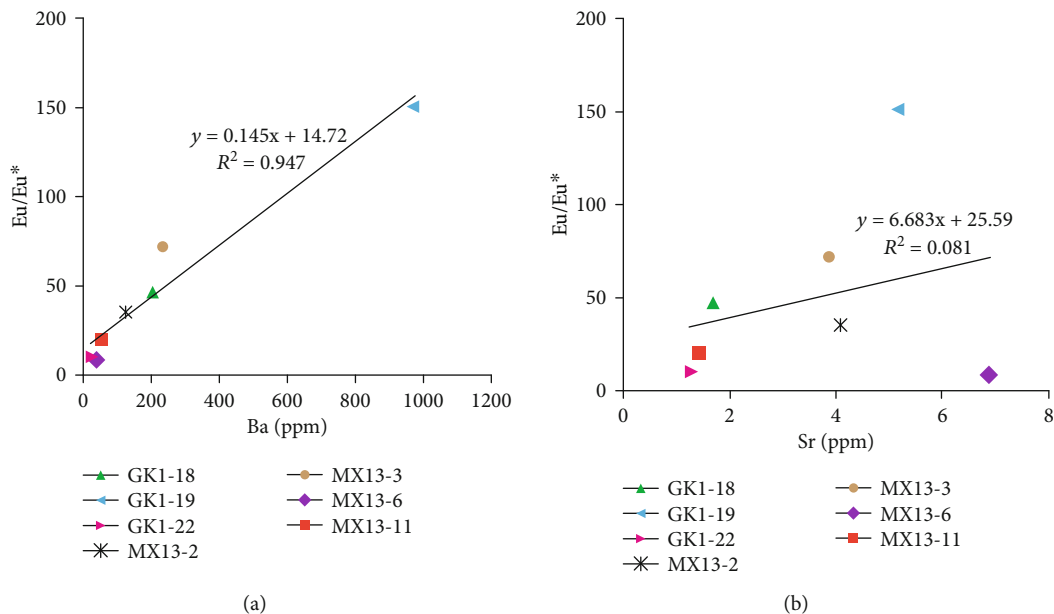


FIGURE 12: Eu/Eu* versus the concentrations of (a) Ba and (b) Sr of the Upper Ediacaran reservoir solid bitumens.

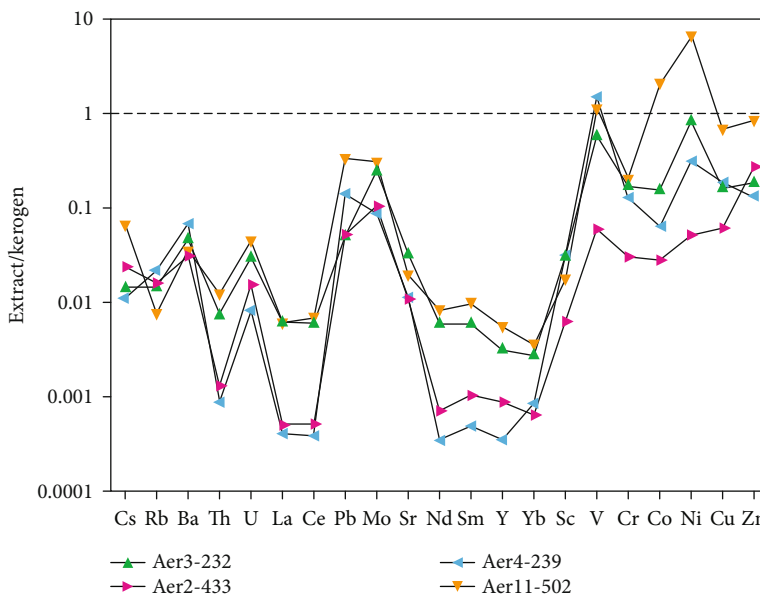


FIGURE 13: Trace elements in extract fraction of mudstones normalized to corresponding kerogen fraction

considered mainly originated from the Lower Cambrian source rocks developed in this intraplatform basin with large thickness and high TOC contents [43, 44]. Consequently, the lowermost Cambrian mudstones with a higher paleoproductivity may be the major origin of Ba enrichment of the Upper Ediacaran reservoir solid bitumens

In a word, although geochemical behaviors of trace elements are very complicated during the formation and evolution of organic matters, the enrichment and mobilization of trace elements in organic fractions of mudstones can still

provide potential information for predicting the distribution characteristics of trace elements in the expelled hydrocarbons of mudstones (e.g., crude oil and solid bitumen) and fingerprinting of oil to source.

6. Conclusion

- (1) Kerogen can be regarded as a special kind of authigenic component in mudstone, and its trace and rare earth elements can be helpful to explore depositional environment of mudstones. In particular, Eu

anomalies of kerogens can be a better indicator of the reducing environment during the sedimentation and early diagenesis of organic matter

- (2) During the oil generation of kerogen, middle rare earth elements (Sm-Ho), especially Eu, migrated from kerogen to extract more easily than the rest REE, and transition metal elements (e.g., Mo, V, Cr, Co, Ni, Cu, and Zn) more easily released from kerogen to extract than the rest elements, especially V and Ni
- (3) The enrichment and mobilization of trace elements (e.g., Mo, U, V, Ni, and Ba) in organic fractions of mudstones are closely related with their geochemical behaviors during the sedimentation and diagenesis, which can provide potential information for predicting the distribution characteristics of trace elements in the expelled hydrocarbons of mudstones (e.g., crude oil and solid bitumen) and fingerprinting of oil to source

Data Availability

The data used to support the findings of this study are included within the article.

Conflicts of Interest

The authors declare that they have no conflicts of interest.

Acknowledgments

We also thank Dr. Meng and Dr. Zhang for spending time in handling our manuscript. This work was funded by the National Natural Science Foundation of China (42030804 and U19B6003-03-01) and the Fundamental Research Funds for the Central Universities (2652019101).

References

- [1] P. A. Abanda and R. E. Hannigan, "Effect of diagenesis on trace element partitioning in shales," *Chemical Geology*, vol. 230, no. 1-2, pp. 42-59, 2006.
- [2] T. J. Algeo and J. B. Maynard, "Trace-element behavior and redox facies in core shales of Upper Pennsylvanian Kansas-type cyclothems," *Chemical Geology*, vol. 206, no. 3-4, pp. 289-318, 2004.
- [3] P. Gao, G. Liu, C. Jia et al., "Redox variations and organic matter accumulation on the Yangtze carbonate platform during Late Ediacaran-Early Cambrian: constraints from petrology and geochemistry," *Palaeogeography, Palaeoclimatology, Palaeoecology*, vol. 450, pp. 91-110, 2016.
- [4] P. Gao, Z. He, S. Li et al., "Volcanic and hydrothermal activities recorded in phosphate nodules from the Lower Cambrian Niutitang Formation black shales in South China," *Palaeogeography, Palaeoclimatology, Palaeoecology*, vol. 505, pp. 381-397, 2018.
- [5] P. Gao, S. Li, G. G. Lash, D. Yan, Q. Zhou, and X. Xiao, "Stratigraphic framework, redox history, and organic matter accumulation of an Early Cambrian intraplatform basin on the Yangtze Platform, South China," *Marine and Petroleum Geology*, vol. 130, article 105095, 2021.
- [6] S. Y. Jiang, H. X. Zhao, Y. Q. Chen, T. Yang, J. H. Yang, and H. F. Ling, "Trace and rare earth element geochemistry of phosphate nodules from the lower Cambrian black shale sequence in the Mufu Mountain of Nanjing, Jiangsu province, China," *Chemical Geology*, vol. 244, no. 3-4, pp. 584-604, 2007.
- [7] B. Jones and D. A. Manning, "Comparison of geochemical indices used for the interpretation of palaeoredox conditions in ancient mudstones," *Chemical Geology*, vol. 111, no. 1, pp. 111-129, 1994.
- [8] F. Martinez-Ruiz, M. Ortega-Huertas, and I. Palomo, "Positive Eu anomaly development during diagenesis of the K/T boundary ejecta layer in the Agost section (SE Spain): implications for trace-element remobilization," *Terra Nova*, vol. 11, no. 6, pp. 290-296, 1999.
- [9] J. L. Morford and S. Emerson, "The geochemistry of redox sensitive trace metals in sediments," *Geochimica et Cosmochimica Acta*, vol. 63, no. 11-12, pp. 1735-1750, 1999.
- [10] R. W. Murray, M. R. B. ten Brink, D. L. Jones, D. C. Gerlach, and G. P. Russ, "Rare earth elements as indicators of different marine depositional environments in chert and shale," *Geology*, vol. 18, no. 3, pp. 268-271, 1990.
- [11] G. Shields and P. Stille, "Diagenetic constraints on the use of cerium anomalies as palaeoseawater redox proxies: an isotopic and REE study of Cambrian phosphorites," *Chemical Geology*, vol. 175, no. 1-2, pp. 29-48, 2001.
- [12] W. Liu, Y. Xu, and J. Chen, "Comprehensive geochemical identification of highly evolved marine carbonate rocks as hydrocarbon-source rocks as exemplified by the Ordos Basin," *Science in China Series D: Earth Sciences*, vol. 49, no. 4, pp. 384-396, 2006.
- [13] N. Tribouillard, T. J. Algeo, T. Lyons, and A. Riboulleau, "Trace metals as paleoredox and paleoproductivity proxies: an update," *Chemical Geology*, vol. 232, no. 1-2, pp. 12-32, 2006.
- [14] D.-H. Pi, C.-Q. Liu, G. A. Shields-Zhou, and S.-Y. Jiang, "Trace and rare earth element geochemistry of black shale and kerogen in the early Cambrian Niutitang Formation in Guizhou province, South China: constraints for redox environments and origin of metal enrichments," *Precambrian Research*, vol. 225, pp. 218-229, 2013.
- [15] B. Liu, A. Bechtel, R. F. Sachsenhofer, D. Gross, R. Gratzner, and X. Chen, "Depositional environment of oil shale within the second member of Permian Lucaogou Formation in the Santanghu Basin, Northwest China," *International Journal of Coal Geology*, vol. 175, pp. 10-25, 2017.
- [16] B. Liu, A. Bechtel, D. Gross, X. Fu, X. Li, and R. F. Sachsenhofer, "Middle Permian environmental changes and shale oil potential evidenced by high-resolution organic petrology, geochemistry and mineral composition of the sediments in the Santanghu Basin, Northwest China," *International Journal of Coal Geology*, vol. 185, pp. 119-137, 2018.
- [17] B. Liu, Y. Song, K. Zhu, P. Su, X. Ye, and W. Zhao, "Mineralogy and element geochemistry of salinized lacustrine organic-rich shale in the Middle Permian Santanghu Basin: implications for paleoenvironment, provenance, tectonic setting and shale oil potential," *Marine and Petroleum Geology*, vol. 120, article 104569, 2020.
- [18] M. Alberdi-Genolet and R. Tocco, "Trace metals and organic geochemistry of the Machiques Member (Aptian-Albian)

- and La Luna Formation (Cenomanian-Campanian),” *Chemical Geology*, vol. 160, no. 1, pp. 19–38, 1999.
- [19] A. Barwise, “Role of nickel and vanadium in petroleum classification,” *Energy & Fuels*, vol. 4, no. 6, pp. 647–652, 1990.
- [20] A. Frankenberger, *Trace Elements in New Zealand Oils, their Significance for Analytical Chemistry, Geochemistry and Oil Classification*, Massey University, 1994, Ph.D dissertation.
- [21] P. Gao, G. Liu, C. Jia et al., “Evaluating rare earth elements as a proxy for oil–source correlation. A case study from Aer Sag, Erlian Basin, northern China,” *Organic Geochemistry*, vol. 87, pp. 35–54, 2015.
- [22] P. Gao, G. Liu, Z. Wang, C. Jia, T. Wang, and P. Zhang, “Rare earth elements (REEs) geochemistry of Sinian–Cambrian reservoir solid bitumens in Sichuan Basin, SW China: potential application to petroleum exploration,” *Geological Journal*, vol. 52, no. 2, pp. 298–316, 2017.
- [23] Q. Jin, H. Tian, and J. Dai, “Application of microelement composition to the correlation of solid bitumen with source rocks,” *Petroleum Geology & Experiment*, vol. 23, no. 3, pp. 285–290, 2001, (in Chinese with English abstract).
- [24] J. Li, S. Zhou, Z. Zheng et al., “REE geochemical characteristics petroleum and gas formation northeastern Sichuan basin,” *Journal of China University of Mining and Technology*, vol. 42, no. 4, pp. 606–615, 2013, (in Chinese with English abstract).
- [25] L. K. Manning, C. D. Frost, and J. Branthaver, “A neodymium isotopic study of crude oils and source rocks: potential applications for petroleum exploration,” *Chemical Geology*, vol. 91, no. 2, pp. 125–138, 1991.
- [26] B. P. Tissot and D. H. Welte, *Petroleum Formation and Occurrence (Second Revised and Enlarged Edition)*, Springer-Verlag, Berlin, Heidelberg, New York, Tokyo, 1984.
- [27] M. J. Hunt, *Petroleum Geochemistry and Geology*, WH Freeman and Company, San Francisco, 1979.
- [28] K. E. Peters, C. C. Walters, and J. M. Moldowan, *The Biomarker Guide*, Cambridge University Press, New York, 2013.
- [29] P. Sundararaman, “On the mechanism of change in DPEP/ETIO ratio with maturity,” *Geochimica et Cosmochimica Acta*, vol. 57, no. 18, pp. 4517–4520, 1993.
- [30] P. Sundararaman and J. E. Dahl, “Depositional environment, thermal maturity and irradiation effects on porphyrin distribution: Alum Shale, Sweden,” *Organic Geochemistry*, vol. 20, no. 3, pp. 333–337, 1993.
- [31] A. J. Finlay, D. Selby, and M. J. Osborne, “Petroleum source rock identification of United Kingdom Atlantic Margin oil fields and the Western Canadian Oil Sands using platinum, palladium, osmium and rhenium: implications for global petroleum systems,” *Earth and Planetary Science Letters*, vol. 313–314, pp. 95–104, 2012.
- [32] W. Jiao, H. Yang, Y. Zhao et al., “Application of trace elements in the study of oil–source correlation and hydrocarbon migration in the Tarim Basin, China,” *Energy Exploration & Exploitation*, vol. 28, no. 6, pp. 451–466, 2010.
- [33] M. McIntire, S. Chaudhuri, M. Totten et al., “Rare earth elements (REEs) in crude oils in the Lansing-Kansas City Formations in Central Kansas: potential indication about sources of the oils, locally derived or long-distance derived,” in *Abstract, AAPG Annual Convention and Exhibition, Houston, Texas, USA, 2014*.
- [34] V. M. Stevanovic and D. Patrick, *Rare earth elements (REE) as a proxy for oil migration: Tyler Formation, North Dakota*. (Abstract) *AAPG Annual Convention and Exhibition, Houston, Texas, USA, 2014*.
- [35] Y. Ren, *Sedimentary Facies and Reservoir Features of Mesozoic in Aer Sag of Erlian Basin. M. S dissertation*, China University of Petroleum (EastChina), 2011, (in Chinese with English abstract).
- [36] X. Zhao, Y. Shi, Y. Zhang, S. Xiang, C. Wu, and F. Jin, *Scientific, Rapid and Efficient Exploration Method and Practice in the New Oil-Rich Sag-a Case from Aer Sag, Erlian Basin*, Science Press, Beijing, 2012, (in Chinese).
- [37] G. Wei, G. Chen, S. Du, L. Zhang, and W. Yang, “Petroleum systems of the oldest gas field in China: Neoproterozoic gas pools in the Weiyuan gas field, Sichuan Basin,” *Sichuan Basin. Marine and Petroleum Geology*, vol. 25, no. 4–5, pp. 371–386, 2008.
- [38] H. Yuan, J. Liang, D. Gong, G. Xu, S. Liu, and G. Wang, “Formation and evolution of Sinian oil and gas pools in typical structures, Sichuan Basin, China,” *Petroleum Science*, vol. 9, no. 2, pp. 129–140, 2012.
- [39] S. Liu, Z. Zhang, W. Huang et al., “Formation and destruction processes of upper Sinian oil-gas pools in the Dingshan-Lintanchang structural belt, Southeast Sichuan Basin, China,” *Petroleum Science*, vol. 7, no. 3, pp. 289–301, 2010.
- [40] P. Gao, G. Liu, G. G. Lash, B. Li, D. Yan, and C. Chen, “Occurrences and origin of reservoir solid bitumen in Sinian Dengying Formation dolomites of the Sichuan Basin, SW China,” *International Journal of Coal Geology*, vol. 200, pp. 135–152, 2018.
- [41] P. Zhang, G. Liu, C. Cai et al., “Alteration of solid bitumen by hydrothermal heating and thermochemical sulfate reduction in the Ediacaran and Cambrian dolomite reservoirs in the Central Sichuan Basin, SW China,” *Precambrian Research*, vol. 321, pp. 277–302, 2019.
- [42] G. Wei, P. Shen, W. Yang et al., “Formation conditions and exploration prospects of Sinian large gas fields,” *Petroleum Exploration and Development*, vol. 40, no. 2, pp. 139–149, 2013.
- [43] Z. Wang, H. Jiang, T. Wang et al., “Paleo-geomorphology formed during Tongwan tectonization in Sichuan Basin and its significance for hydrocarbon accumulation,” *Petroleum Exploration and Development*, vol. 41, no. 3, pp. 338–345, 2014.
- [44] C. Zou, J. Du, C. Xu et al., “Formation, distribution, resource potential, and discovery of Sinian-Cambrian giant gas field, Sichuan Basin, SW China,” *Petroleum Exploration and Development*, vol. 41, no. 3, pp. 306–325, 2014.
- [45] H. R. Rollison, *Using Geochemical Data: Evaluation, Presentation, Interpretation*. Longan Scientific & Technical, New York, 1993.
- [46] S. M. McLennan, “Chapter 7. Rare earth elements in sedimentary ROCKS: influence of provenance and sedimentary processes,” *Reviews in Mineralogy and Geochemistry*, vol. 21, no. 1, pp. 169–200, 1989.
- [47] H. Jacob, “Disperse solid bitumens as an indicator for migration and maturity in prospecting for oil and gas,” *Erdöl & Kohle, Erdgas, Petrochemie*, vol. 38, no. 8, p. 365, 1985.
- [48] S. M. McLennan, “Relationships between the trace element composition of sedimentary rocks and upper continental crust,” *Geochemistry, Geophysics, Geosystems*, vol. 2, no. 4, p. 2000GC000109, 2001.
- [49] X. Ding, G. Liu, Z. Huang, M. Sun, Z. Chen, and X. Liu-zhuang, “The impact on organic matter

- preservation by the degree of oxidation and reduction and sedimentation rates of Erlian basin,” *Natural Gas Geoscience*, vol. 25, no. 6, pp. 810–817, 2014, (in Chinese with English abstract).
- [50] G. Eskenazy, “Aspects of the geochemistry of rare earth elements in coal: an experimental approach,” *International Journal of Coal Geology*, vol. 38, no. 3–4, pp. 285–295, 1999.
- [51] W. Wang, Y. Qin, S. Sang, Y. Zhu, C. Wang, and D. J. Weiss, “Geochemistry of rare earth elements in a marine influenced coal and its organic solvent extracts from the Antaibao mining district, Shanxi, China,” *International Journal of Coal Geology*, vol. 76, no. 4, pp. 309–317, 2008.
- [52] R. Pelet, F. Behar, and J. C. Monin, “Resins and asphaltenes in the generation and migration of petroleum,” *Organic Geochemistry*, vol. 10, no. 1–3, pp. 481–498, 1986.
- [53] S. Felitsyn and S. Morad, “REE patterns in latest Neoproterozoic-early Cambrian phosphate concretions and associated organic matter,” *Chemical Geology*, vol. 187, no. 3–4, pp. 257–265, 2002.
- [54] C.-P. Wong, R. F. Venteicher, and W. D. Horrocks Jr., “Lanthanide porphyrin complexes. Potential new class of nuclear magnetic resonance dipolar probe,” *Journal of the American Chemical Society*, vol. 96, no. 22, pp. 7149–7150, 1974.
- [55] S. Radzki, P. Krausz, S. Gaspard, and C. Giannotti, “A study of complex formation between differently charged free-base porphyrins and samarium porphyrins,” *Inorganica Chimica Acta*, vol. 138, no. 2, pp. 139–143, 1987.
- [56] Q. Chen and G. Chen, *Practical REE Geochemistry*, Metallurgical Industry Press, Beijing, 1990, (in Chinese).
- [57] P. Henderson, *Rare Earth Element Geochemistry*, Elsevier, Amsterdam, 1984.
- [58] N. D. MacRae, H. W. Nesbitt, and B. I. Kronberg, “Development of a positive Eu anomaly during diagenesis,” *Earth and Planetary Science Letters*, vol. 109, no. 3–4, pp. 585–591, 1992.
- [59] L. Chen, *Sedimentology and Geochemistry of the Early Cambrian Black Rock Series in the Hunan-Guizhou Area, China*, Ph.D dissertation, Institute of Geochemistry, Chinese Academy of Sciences, 2006.
- [60] R. Shannon, “Revised effective ionic radii and systematic studies of interatomic distances in halides and chalcogenides,” *Acta Crystallogr. Sect. A*, vol. 32, no. 5, pp. 751–767, 1976.
- [61] P. Dulski, “Interferences of oxide, hydroxide and chloride anolyte species in the determination of rare earth elements in geological samples by inductively coupled plasma-mass spectrometry,” *Fresenius’ Journal of Analytical Chemistry*, vol. 350, no. 4–5, pp. 194–203, 1994.
- [62] H. Zhang, L. Zhou, J. Wang, J. Su, L. Cao, and M. Dai, “Molybdenum isotopic compositions and significance of bitumen at different geological periods in Shangsi section, Guangyuan, Sichuan,” *Earth Science - Journal of China University of Geosciences*, vol. 36, no. 6, pp. 1053–1063, 2011, (in Chinese with English abstract).
- [63] S. Jiang, J. Yang, H. Ling, H. Feng, Y. Chen, and J. Chen, “Re-Os isotopes and PGE geochemistry of black shales and intercalated Ni-Mo polymetallic sulfide bed from the lower Cambrian Niutitang Formation, South China,” *Progress in Natural Science*, vol. 13, no. 10, pp. 788–794, 2003.
- [64] S. M. McLennan and S. Taylor, “Th and U in sedimentary rocks: crustal evolution and sedimentary recycling,” *Nature*, vol. 285, no. 5767, pp. 621–624, 1980.
- [65] J. H. Patterson, L. S. Dale, J. J. Fardy, and A. R. Ramsdent, “Characterization of trace elements in rundle and condor oil shales,” *Fuel*, vol. 66, no. 3, pp. 319–322, 1987.
- [66] P. Halbach, D. Von Borstel, and K.-D. Gundermann, “The uptake of uranium by organic substances in a peat bog environment on a granitic bedrock,” *Chemical Geology*, vol. 29, no. 1–4, pp. 117–138, 1980.
- [67] R. Nakada, Y. Takahashi, G. Zheng, Y. Yamamoto, and H. Shimizu, “Abundances of rare earth elements in crude oils and their partitions in water,” *Geochemical Journal*, vol. 44, no. 5, pp. 411–418, 2010.
- [68] W. S. Broecker and T.-H. Peng, *Tracers in the Sea*, Eldigio Press, New York, 1982.
- [69] H.-J. Brumsack, “Geochemistry of recent TOC-rich sediments from the Gulf of California and the Black Sea,” *Geologische Rundschau*, vol. 78, no. 3, pp. 851–882, 1989.
- [70] S. Calvert and T. Pedersen, “Geochemistry of recent oxic and anoxic marine sediments: implications for the geological record,” *Marine Geology*, vol. 113, no. 1–2, pp. 67–88, 1993.
- [71] T. P. Vorlicek, M. D. Kahn, Y. Kasuya, and G. R. Helz, “Capture of molybdenum in pyrite-forming sediments: role of ligand-induced reduction by polysulfides¹,” *Geochimica et Cosmochimica Acta*, vol. 68, no. 3, pp. 547–556, 2004.
- [72] S. Calvert and D. Piper, “Geochemistry of ferromanganese nodules from DOMES Site A, Northern Equatorial Pacific: multiple diagenetic metal sources in the deep sea,” *Geochimica et Cosmochimica Acta*, vol. 48, no. 10, pp. 1913–1928, 1984.
- [73] G. N. Breit and R. B. Wanty, “Vanadium accumulation in carbonaceous rocks: a review of geochemical controls during deposition and diagenesis,” *Chemical Geology*, vol. 91, no. 2, pp. 83–97, 1991.
- [74] D. Piper and R. Perkins, “A modern vs. Permian black shale—the hydrography, primary productivity, and water-column chemistry of deposition,” *Chemical Geology*, vol. 206, no. 3–4, pp. 177–197, 2004.
- [75] M. Lewan and J. Maynard, “Factors controlling enrichment of vanadium and nickel in the bitumen of organic sedimentary rocks,” *Geochimica et Cosmochimica Acta*, vol. 46, no. 12, pp. 2547–2560, 1982.
- [76] R. H. Fish, J. J. Komlenic, and B. K. Wines, “Characterization and comparison of vanadyl and nickel compounds in heavy crude petroleum and asphaltenes by reverse-phase and size-exclusion liquid chromatography/graphite furnace atomic absorption spectrometry,” *Analytical Chemistry*, vol. 56, no. 13, pp. 2452–2460, 1984.
- [77] Y. Zheng, R. F. Anderson, A. van Geen, and M. Q. Fleisher, “Remobilization of authigenic uranium in marine sediments by bioturbation,” *Geochimica et Cosmochimica Acta*, vol. 66, no. 10, pp. 1759–1772, 2002.
- [78] J. McManus, W. M. Berelson, G. P. Klinkhammer, D. E. Hammond, and C. Holm, “Authigenic uranium: relationship to oxygen penetration depth and organic carbon rain,” *Geochimica et Cosmochimica Acta*, vol. 69, no. 1, pp. 95–108, 2005.
- [79] J. Dymond, E. Suess, and M. Lyle, “Barium in deep-sea sediment: a geochemical proxy for paleoproductivity,” *Paleoceanography*, vol. 7, no. 2, pp. 163–181, 1992.
- [80] P. Emsbo, A. H. Hofstra, C. A. Johnson et al., “Lower Cambrian metallogenesis of South China: interplay between diverse basinal hydrothermal fluids and marine chemistry,” in *Mineral Deposit Research: Meeting the Global Challenge*, J. Mao and F.

P. Bierlein, Eds., pp. 115–118, Proceedings of the Eighth Biennial SGA Meeting Beijing, Springer, Berlin, 2005.

- [81] P. W. Jewell, “Bedded barite in the geologic record,” in *Marine Authigenesis: From Global to Microbial*, *SEPM Special Publication*, C. R. Glenn and L. J. Prevot-Lucus, Eds., vol. 66 of No, pp. 161–174, 2000.
- [82] S. Li, P. Gao, B. Huang, H. Wang, and Y. Wo, “Sedimentary constraints on the tectonic evolution of Mainyang-Changning trough in the Sichuan Basin,” *Oil and Gas Geology*, vol. 39, pp. 889–898, 2018, (in Chinese with English abstract).